



Multifunctional degradable electronic scaffolds for cardiac tissue engineering

Ron Feiner^{a,b,1}, Sharon Fleischer^{a,b,1}, Assaf Shapira^{a,b}, Or Kalish^a, Tal Dvir^{a,b,c,d,*}

^a The School for Molecular Cell Biology and Biotechnology, Faculty of Life Sciences, Tel Aviv University, Tel Aviv 69978, Israel

^b The Center for Nanoscience and Nanotechnology, Tel Aviv University, Tel Aviv 69978, Israel

^c Department of Materials Science and Engineering, Faculty of Engineering, Tel Aviv University, Tel Aviv 69978, Israel

^d Sagol Center for Regenerative Biotechnology, Tel Aviv University, Tel Aviv 69978, Israel



ARTICLE INFO

Keywords:

Cardiac tissue engineering
Electronic scaffold
Controlled release

ABSTRACT

The capability to on-line sense tissue function, provide stimulation to control contractility and efficiently release drugs within an engineered tissue microenvironment may enhance tissue assembly and improve the therapeutic outcome of implanted engineered tissues. To endow cardiac patches with such capabilities we developed elastic, biodegradable, electronic scaffolds. The scaffolds were composed of electrospun albumin fibers that served as both a substrate and a passivation layer for evaporated gold electrodes. Cardiomyocytes seeded onto the electronic scaffolds organized into a functional cardiac tissue and their function was recorded on-line. Furthermore, the electronic scaffolds enabled to actuate the engineered tissue to control its function and trigger the release of drugs. Post implantation, these electronic scaffolds degraded, leading to the dissociation of the inorganic material from within the scaffold. Such technology can be built upon to create a variety of degradable devices for tissue engineering of various tissues, as well as pristine cell-free devices with electronic components for short-term *in vivo* use.

1. Introduction

Cardiac patches are considered a promising approach for regenerating the infarcted heart. However, once the 3D cardiac patches have been engineered, proper *in vitro* assessment of their quality in terms of electrical activity without affecting their performance is limited. This may lead to implantation of cardiac patches with limited or no potential to integrate and synchronize with the healthy tissue surrounding the infarct, jeopardizing the efficacy of the treatment.

Recent studies have advanced the field of cardiac tissue engineering by integrating flexible electronic components within the 3D scaffolds to allow monitoring and actuation of tissue performance [1–3]. These electronic meshes were highly porous and allowed the seeded cardiomyocytes to organize into a confluent 3D tissue. Using these devices, it was possible to monitor cardiac tissue performance and response to drugs at different locations, control the pace and direction of signal propagation, and release drugs and proteins from within electroactive polymers deposited onto the electrodes. This work adds to the existing body of work on drug delivery in cardiac disease [4–6].

While these hybrid tissues represent a significant step forward, their electronics are fabricated from relatively rigid, synthetic substrates

such as SU-8 or polyimide that do not undergo *in-vivo* degradation. However, when the electronics' function is only needed for the short-term *in vitro* phase or for the initial integration period inside the host, degradation of the electronic components is advantageous. In order to address this issue, many natural substrates such as silk [7,8], collagen [9] and paper [10], have been used. Other synthetic materials, such as poly(caprolactone), poly(lactic-co-glycolic) acid and polylactic acid have also been used as substrates for transient silicon electronic devices [11]. However, these devices were all fabricated on continuous substrate films, which do not allow for proper 3D tissue organization.

Recently, a blend of poly(caprolactone) and poly(glycerol sebacate) was electrospun to create a nanofibrous, flexible, degradable substrate. By using screen printing of silver paste, electrodes were defined onto the substrate and their use as heat and strain sensors was demonstrated [12]. However, these materials were not used to control engineered tissue function or the host's microenvironment.

Here, we sought to engineer a 3D biodegradable scaffold for cardiac tissue engineering with integrated electronics. In this approach, gold electrodes are directly deposited on an electrospun fiber scaffold. An additional electrospun fiber layer is incorporated on top of the electrodes, serving as a passivation layer and exposing only defined areas

* Corresponding author at: The School for Molecular Cell Biology and Biotechnology, Faculty of Life Sciences, Tel Aviv University, Tel Aviv 69978, Israel.

E-mail address: tdvir@post.tau.ac.il (T. Dvir).

¹ These authors contributed equally to this work.

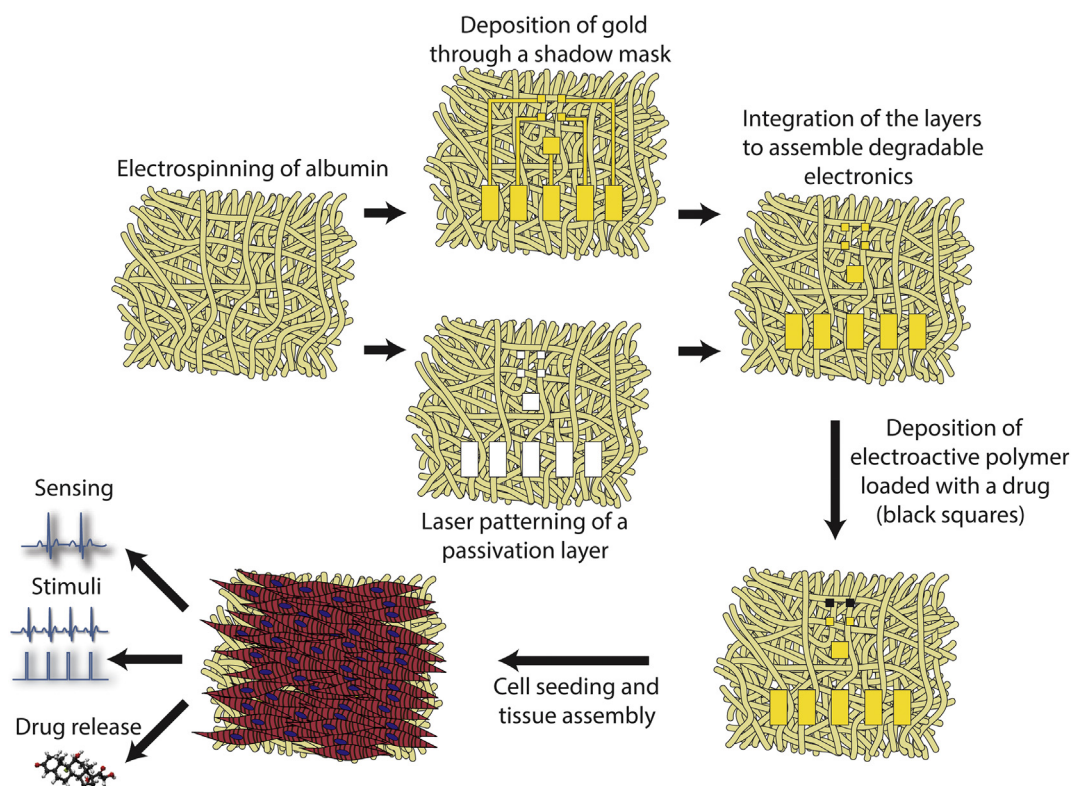


Fig. 1. Process schematics. Albumin is electrospun into two thick mats. The first mat is covered with a shadow masks and 600 nm thick Au electrodes are evaporated onto it. The second mat is used as a passivation layer; holes specific to the electrode pad locations are defined using laser patterning. The two layers are assembled into a complete device using an ECM-based hydrogel as an adhesive. Following, a layer of polypyrrole loaded with dexamethasone is deposited onto selected electrodes. Finally, neonatal rat ventricular cardiomyocytes are seeded onto the device and are allowed to organize into a functional cardiac tissue. By connecting the device to an external amplifier, extracellular signals may be recorded from the tissue and stimuli may be delivered to the device for pacing and drug release.

on the electrodes. We demonstrate that the electronic scaffolds are stretchable and flexible and support the contraction of an engineered cardiac tissue. The electronic component within can sense the function of the engineered tissue, provide electrical stimulation for pacing and release anti-inflammatory drugs (Fig. 1). Moreover, we show that the scaffolds can degrade *in vivo* after implantation.

2. Materials and methods

2.1. Electrospinning albumin fiber scaffolds

Bovine serum albumin [Fraction V, 14% (wt/vol)] (MP biomedical) was dissolved in tetrafluoroethylene (TFE) and distilled water (9:1) overnight. The following day, 2.5% (vol/vol) β -mercaptoethanol (Merck) was added for overnight mixing. The solution was electrospun at room temperature using a syringe pump (Harvard Apparatus) at a rate of 1 mL/h through a 20G needle. A high voltage power supply (Glassman High Voltage) was used to apply a 12 kV potential between the needle tip of the syringe and the grounded aluminum collector placed at a distance of 14 cm from the needle.

2.2. Pore size and fiber diameter analysis

SEM images were taken and images were analyzed using ImageJ software.

2.3. Shadow mask and passivation layer micropatterning

A Master-Femto femtosecond laser micromachining system (ELAS, Ltd.) was used for the micropatterning of albumin fiber scaffolds (1026 nm, 1–5 W, 150 Hz) and plastic sheet shadow masks. Several

10 μ L drops of ECM glue were placed on top of the bottom scaffold and the passivation layer scaffold was placed on top of it. The scaffolds were then incubated for 30 min in 37 °C in order for the gel to solidify.

2.4. Gold electrode deposition

One hundred micrometre thick albumin fiber sheets covered by the plastic shadow mask were mounted in a VST e-beam evaporator (VST, Petah Tikva, Israel). Au (99.999%) was evaporated from a tungsten boat at $1\text{--}3 \times 10^{-6}$ Torr at a deposition rate of 2.5 A s^{-1} .

2.5. In-vitro degradation

Gold coated devices were weighed and placed in phosphate buffered saline at 37 °C and 5% CO_2 . Every seven days devices were taken out, blotted dry and weighed.

2.6. Scanning electron microscopy

Samples were mounted onto aluminum stubs with conductive paint and were sputter-coated with an ultrathin (150 Å) layer of gold in a Polaron E5100 coating apparatus (Quorum Technologies). The samples were viewed under a JCM-6000PLUS NeoScope Benchtop scanning electron microscope (JEOL USA, Inc.).

2.7. Electrical resistance measurements

All measurements of conductivity were performed using a Keithley DMM-7510 multimeter (Keithley Instruments, Cleveland, OH) using a two probe setup.

2.8. Mechanical testing

Albumin fiber scaffolds (Pristine or covered by a 600 nm Au layer) were cut into 1×5 cm rectangular strips and were tested using a model LS1 tensile testing instrument (Lloyd Instruments, Ltd.) with a 5 N load cell at a rate of 10 mm/min.

2.9. Cardiac cell isolation, seeding and cultivation

Cardiac cells were isolated according to Tel Aviv University ethical use protocols as previously described [1]. Briefly, left ventricles of 0–3-day-old neonatal Sprague–Dawley rats (Harlan Laboratories, Israel) were harvested, and cells were isolated using six cycles (30 min each at 37 °C) of enzyme digestion with collagenase type II (95 U/mL; Worthington, Lakewood, NJ) and pancreatin (0.6 mg/mL; Sigma–Aldrich) in Dulbecco's modified Eagle Medium (DMEM, CaCl₂·2H₂O (1.8 mM), KCl (5.36 mM), MgSO₄·7H₂O (0.81 mM), NaCl (0.1 M), NaHCO₃ (0.44 mM), NaH₂PO₄ (0.9 mM)). After each round of digestion cells were centrifuged (600G, 5 min) and resuspended in culture medium composed of M-199 supplemented with 0.6 mM CuSO₄·H₂O, 0.5 mM ZnSO₄·7H₂O, 1.5 mM vitamin B12, 500 U/mL Penicillin and 100 mg/mL streptomycin, and 0.5% (v/v) FBS (Biological industries, Israel). To enrich the cardiomyocyte population, cells were suspended in culture medium with 5% FBS and pre-plated twice (45 min). Cell number and viability was determined by a hemocytometer and a trypan blue exclusion assay.

2.10. Immunostaining

Cell constructs were fixed and permeabilized in 100% cold methanol for 10 min, washed three times in PBS buffer, and then blocked for 1 h at room temperature in DMEM-based buffer containing 2% (vol/vol) fetal bovine serum (FBS). The samples were then washed three times in PBS. Cardiac tissues were incubated with primary mouse anti- α -sarcomeric actinin antibody (1:750) (Sigma–Aldrich), washed three times, and incubated for 1 h with Alexa Fluor 647-conjugated goat anti-mouse antibody (1:500) (Jackson). For nuclei detection, the cells were incubated for 3 min with Hoechst 33258 (5 μ g/mL) (Sigma) and were washed three times. Samples were visualized using a scanning laser confocal microscope (Nikon Eclipse Ni).

2.11. Extracellular potential recordings

The devices were connected to an AM systems differential AC amplifier Model 1700 and then to a USB X series multifunction data acquisition system (National Instruments). Extracellular potentials were recorded using LabView Signal Express software.

2.12. Calcium imaging

Constructs were incubated with 10 μ M fluo-4 AM (Invitrogen) and 0.1% Pluronic F-127 (Sigma–Aldrich) for 45 min at 37 °C. Constructs were washed in medium and imaged using an inverted fluorescent microscope (Nikon Eclipse TI). Videos were acquired with an ORCA-Flash 4.0 digital complementary metal-oxide semiconductor (CMOS) camera (Hamamatsu Photonics) at 100 frames/s using NIS-Elements software (Nikon). Electrical signal propagation was measured by ImageJ (NIH). Stimulation was performed using a Multichannel Systems STG-4002 stimulus generator. Pacing was performed by applying 1–3 V, 50 ms long pulses at 1–2 Hz.

2.13. Dexamethasone release from polypyrrole films

PPy/DEX films were grown potentiostatically onto the device electrodes using a Bio-Logic SP-150 potentiostat. The electro-synthesis solution consisted of 0.2 M Pyrrole (Alfa Aesar, Ward Hill, MA) and 0.1 M

DEX (Sigma–Aldrich, dexamethasone 21 phosphate disodium, used as received) in Milli-Q water of 18 M Ω /cm resistivity. The film was synthesized by applying a constant potential of 1 V for 10 min between the device and a counter electrode. For drug release experiments, the counter and working electrodes were reversed. The amount of released DEX was quantified by absorbance at 242 nm (a characteristic band of DEX) using an infinite M200 Pro plate reader (TECAN).

2.14. The effect of released DEX on NO production in macrophages

RAW 264.7 cells (ATCC) were cultured at 37 °C in a humidified, 5% carbon dioxide atmosphere in DMEM (without phenol red) supplemented with 10% (vol/vol) heat-inactivated FBS, 100 U/mL penicillin, 100 μ g/mL streptomycin, and 2 mM L-glutamine (Biological Industries, Israel). RAW 264.7 cells (6.4×10^4 , in a total volume of 80 μ L) were seeded in the wells of a 96-well plate. Seven hours later, the cells were supplemented with an additional 10 μ L of medium without or with the released DEX. Twenty-four hours later, 10 μ L of growth medium containing 1000 ng/mL of LPS (L4391, Sigma Aldrich) was added to each well, reaching a final concentration of 100 ng/mL. After a 24 h incubation, 50 μ L samples of cell growth medium were analyzed for nitrite concentration (used as an indicator of NO production) using Griess reagent (Promega). Cell viability was determined by a presto blue assay ($n \geq 6$ in each group).

2.15. In vivo implantation and histology

Recipient SD male rats (150–200 g) (Envigo Laboratories) were anesthetized using a combination of ketamine (40 mg/kg) and xylazine (10 mg/kg) according to Tel Aviv University ethical use protocols. Samples were implanted S.C. by creating a small incision on the rat's back. Scaffolds were inserted into the cavity created by the incision. Rats were killed 1 or 3 weeks after implantation, and the samples were extracted, fixed in formalin and embedded in OCT. Sections (10 μ m thick) were prepared using a cryotome. Samples were visualized using a stereomicroscope (Nikon SMZ18).

2.16. Statistical analysis

Statistical analysis data are presented as means \pm SEM. Differences between samples were assessed by a Student's *t*-test. All analyses were performed using GraphPad Prism version 6.00 for Windows (GraphPad Software). $P < 0.05$ was considered significant.

3. Results and discussion

Electrospun fibrous scaffolds composed of bovine serum albumin were chosen as the substrate and dielectric material for the devices. These scaffolds display mechanical and biochemical properties that promote cardiac tissue organization [13]. As albumin is a natural biocompatible protein, it can be degraded into smaller peptides within the body by proteolytic enzymes while its degradation *in-vitro* does not occur or is undetectable (Fig. S1) [14].

Gold is a biocompatible, inert metal, which has been widely used to fabricate stretchable and implantable electronics [15–17]. In addition, its potential to improve the organization and function of engineered cardiac tissues when used in conjugation with electrospun scaffolds has been previously demonstrated [18–21]. In order to add electrodes that enable sensing and actuating elements to our scaffolds, and trigger drug release from electroactive polymers, 600 nm thick gold electrodes were evaporated onto ~ 100 μ m thick albumin fiber scaffolds, using e-beam evaporation and a custom designed shadow mask (Fig. 2A). Such gold deposition did not affect the elastic modulus of the albumin fiber scaffolds (Fig. S2). As a proof of concept, the device was composed of four sensing/stimulating electrodes ending with 1 mm² square pads and a 1 mm spacing between them. One large, 9 mm² electrode served as a

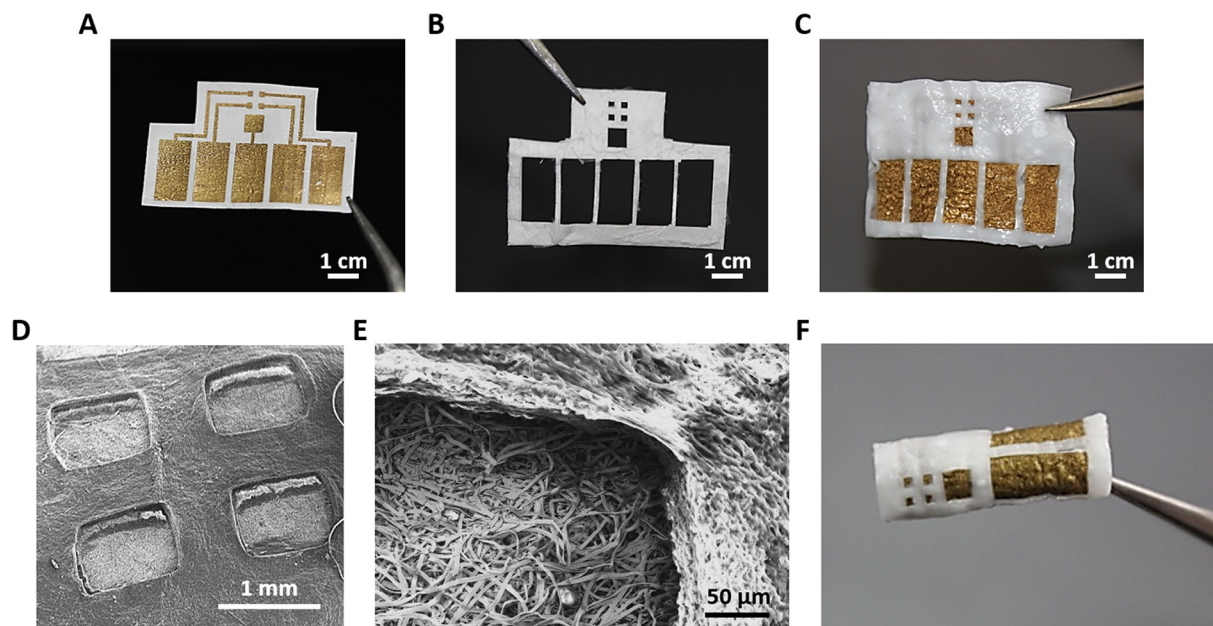


Fig. 2. Electronic scaffold fabrication. (A) Gold electrodes deposited onto the electrospun albumin-fiber scaffold. The electrodes are defined using a shadow mask. (B) Electrospun albumin-fiber scaffold defined into a passivation layer using laser patterning. (C) A complete device composed of a bottom electrode layer and a top passivation layer. Both layers are glued together using an ECM-based hydrogel. (D) Scanning electron micrograph of all four sensing/stimulating electrodes. (E) Scanning electron micrograph of the interface between the bottom electrode layer and the top passivation layer. (F) A complete electronic scaffold rolled into a tube.

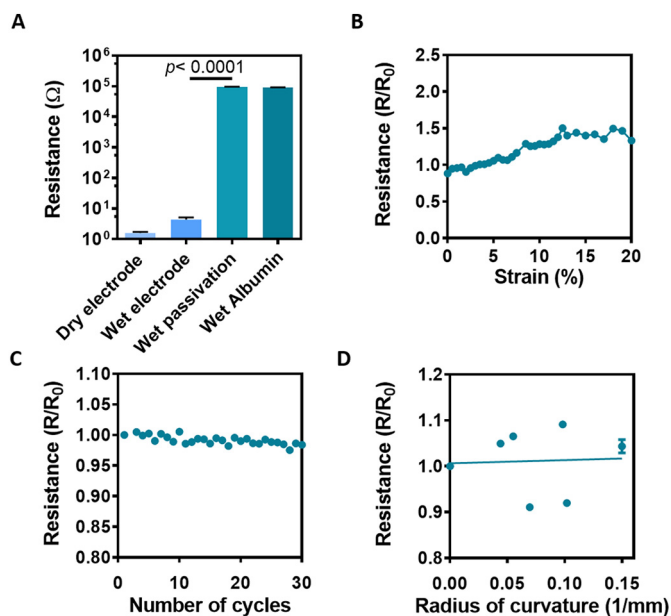


Fig. 3. Electrical characterization of the scaffolds. (A) Electrical resistance along the defined Au electrodes and the passivation layer in dry and wet conditions. Wet passivation describes the layer of albumin fibers covering the gold wires directly. (B) Electrical resistance as a function of mechanical strain of the fabricated scaffolds. (C) Electrical resistance as a function of cyclical strain. (D) Electrical resistance as a function of radius of curvature imposed on the electronic scaffold.

ground electrode for recording and stimulation (Fig. 2A). To ensure that signal recording or stimulation will occur only at the desired location and not throughout the electrodes, a passivation layer, covering the electrodes is needed. Here, passivation of the electrodes was achieved using a second laser-patterned albumin fiber scaffold designed to leave the functional pads exposed (Fig. 2B) [22]. After both components of the device have been fabricated, they were glued together using a

thermoresponsive ECM-based hydrogel, which is liquid in room temperature and solidifies in 37 °C (Fig. 2C) [23]. Scanning electron micrographs revealed a clear height difference between the bottom electrode layer and the top passivation layer (Fig. 2D and E). The final device was thick and robust and could be easily manipulated, folded and rolled for creating thicker tissues (Fig. 2F).

The albumin fiber scaffold is highly porous, exhibiting an average pore size of $335.4 \pm 58.85 \mu\text{m}^2$ and an average fiber diameter of $3.616 \pm 0.596 \mu\text{m}$. As such these scaffolds allow for efficient gas and nutrient exchange [22]. While these properties are very useful for tissue engineering, we sought to ensure that there were no current leaks from the bottom electrode layer and through the top passivation layer. Towards that end, we performed a two-wire resistance measurement between different locations on the device (Fig. 3A). Resistance between two exposed gold pads connected by a passivated gold wire was $\sim 5 \Omega$ when the device was placed in phosphate buffer saline (PBS) and around 1.5Ω when dry. Resistance measured between one exposed gold pad and a passivated part of the gold wire connected to it in PBS was 5 orders of magnitude higher ($\sim 10^5 \Omega$). The same resistance ($\sim 10^5 \Omega$) was measured between two locations on the pristine albumin fiber scaffold (Fig. 3A). This resistance could be attributed to the saline solution in which the device is placed during measurement, as the resistance between two locations on the pristine albumin fiber scaffold when dry was infinite.

To further characterize the devices, their ability to withstand continuous contractions as those of the heart was investigated. Changes in resistance were measured as a function of applied cyclic strain. Cardiac sarcomere extension can reach up to 20%, while changes in volume between systole and diastole in the cardiac cycle can reach 10% [24–26]. Our results showed a change of $\sim 30\%$ in conductivity when the devices were stretched to 20% strain (Fig. 3B). When cyclically stretched the scaffolds showed no change in conductivity for at least 30 cycles (Fig. 3C). In addition, no structural failures were detectable in the fibers when examined under scanning electron microscopy (Fig. S3). To demonstrate the flexibility of our devices while keeping the electrodes intact, they were wrapped around cylinders with decreasing diameters and electrode resistance was measured. Our results revealed that the conductivity of the devices remained constant and no

significant increase in resistance was measured (Fig. 3D). Taken together, these results demonstrate the flexibility and elasticity of the electronic scaffold. Such mechanical properties allow the scaffolds to adapt to the topography of their target organ, and withstand the motions and stress exerted on it, while preserving their electrical properties.

We next sought to evaluate the ability of the electronic component within the scaffold to support tissue growth and regulate engineered tissue function. Cardiomyocytes were isolated from the ventricles of neonatal rats and seeded within the electronic scaffolds. Seven days post seeding, the engineered tissues were fixed and stained for α -actinin, revealing massive striation and an aligned morphology of the cells, both on the electrodes and the pristine part of the scaffold (Fig. 4A and B), indicating on the assembly of the tissue and its maturation.

One of the challenges of cardiac tissue engineering is monitoring tissue integration and function. Endowing the cardiac patch with this ability may help alert the physician of a potential failure in patch function or integration. Thus, we initially sought to evaluate the ability of the electronic scaffolds to serve as a sensor for tissue function. The engineered tissues were connected to an external amplifier and extracellular potentials were recorded from within the tissue. The pace of spontaneous contractions evaluated through these recordings was ~ 0.8 Hz (Fig. 4C). To demonstrate our capability to control cardiac tissue contraction through the device, the engineered tissues were placed on ice to reduce spontaneous contractions. Following, the electrodes were connected to an external stimulus generator, and a 50 ms, 1 V pulse was delivered to a specific electrode at a 1 or 2 Hz pace. Calcium imaging was used to validate tissue contraction in response to stimulation. Contractions were observed at the applied pace and ceased when no stimulation was applied, indicating on our ability to remotely manipulate tissue function (Fig. 4D and Supplementary Video S1).

Another major challenge in tissue engineering is the immune reaction following implantation. Immune response may lead to rejection of the implant and thus, may jeopardize the treatment and the patient's health. In order to reduce inflammation after transplantations, anti-inflammatory drugs are administered. To extend the period of immune abatement we incorporated a drug release system into the device and chose to release the anti-inflammatory drug dexamethasone (DEX). DEX is widely used when implanting biomedical devices or other grafts to reduce the inflammatory response and improve the therapeutic outcome [27]. To allow proper control over the release of the drug, we sought to exploit the ability of the electronic scaffold to deliver voltage through the designed electrodes. Thus, an electroactive polymer was incorporated into the system, for efficient controlled release of negatively-charged drugs. A layer of polypyrrole (PPy) loaded with a negatively charged derivative of DEX was deposited onto a gold electrode with a loading efficiency of $8.32 \pm 2.6\%$ by applying a constant voltage of 1 V (Fig. 5A–C). DEX release could be achieved by reversing the poles of the applied electric field (Fig. 5D). This system is intended for a single drug administration. However, it is possible to deposit polypyrrole with the loaded drug on several electrodes and release it at different time points. In addition, the device can be tailored so that there are as many drug-loaded electrodes as needed. To evaluate that the released DEX retains its potential to reduce inflammation, LPS activated macrophages were exposed to the released drug. The macrophages showed a significantly reduced amount of nitric oxide (NO) secretion, a molecule secreted during inflammation (Fig. 5D). Potentially, other negatively charged drugs or biofactors, such as acetylsalicylic acid, heparin or amiodarone could be loaded within the PPy layer and released into the vicinity of the device to ameliorate the effects of implantation or improve tissue function.

Finally, the *in vivo* degradation of the devices was assessed. The devices were folded to better imitate a thick 3D tissue representing the human ventricle. In this manner, the electrodes are dispersed between several distinct layers. The folded devices were implanted in adult rats subcutaneously (Fig. 6A), and were extracted after 1 or 3 weeks.

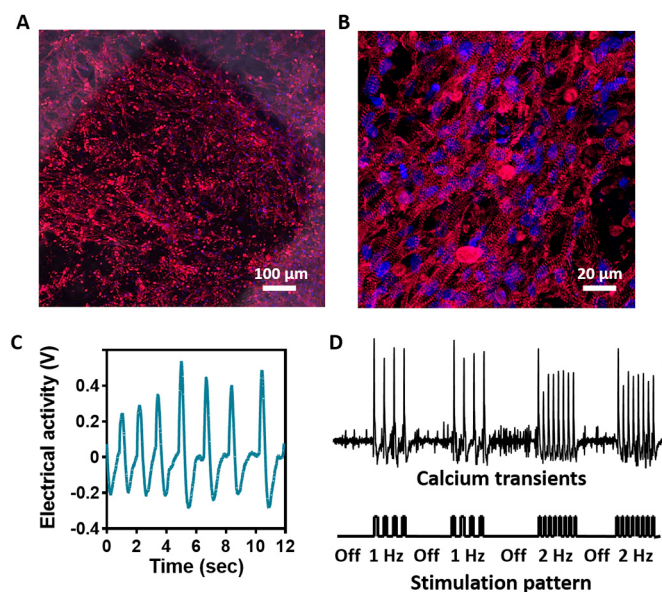


Fig. 4. Tissue organization and function within the electronic scaffold. (A) Confocal microscope image showing the assembled cardiac tissue on and around the Au electrode. Red - sarcomeric actinin, blue - nuclei. (B) Zoomed-in image of cardiac cells revealing elongated cells and a massive striation. (C) Extracellular signals recorded from a sensing electrode within the electronic scaffold. (D) Calcium transients recorded as a function of stimulation through the electronic scaffold. (For interpretation of the references to colour in this figure legend, the reader is referred to the web version of this article.)

Scaffolds that were extracted after one week showed early signs of degradation but were mostly left intact with dimensions of $\sim 1 \times 1.7$ cm (Fig. 6B). Scaffolds that were extracted 3 weeks post implantation showed advanced signs of degradation with dimensions of $\sim 0.7 \times 0.8$ cm (Fig. 6C). Thin sections of the extracted scaffolds revealed that after one week the devices remained intact, with a clear electronic layer (Fig. 6D). Three weeks after implantation, the biomaterial has degraded, dissociating the electronics within to small fragments (Fig. 6E). Image analysis of the implants' sections revealed a significant increase in the degraded area 3 weeks post implantation with a remaining area of $< 50\%$ (Fig. 6H). These results show that our technology can be used for transient electronic implants. After the devices have served their purpose, their function will be eliminated and they will be naturally degraded.

4. Conclusion

Cardiac tissue engineering aims at replacing the damaged scar tissue left after myocardial infarction. Once this replacement tissue has been engineered, it is difficult to monitor its integration and function *in vivo*. By integrating electronic components into the engineered tissue, monitoring and controlling its function can be achieved. We have described here the fabrication of a flexible, degradable and biocompatible electronic scaffold for cardiac tissue engineering. This device maintained its conductivity following extensive manipulations and was able to promote the assembly of 3D cardiac tissues. Using the deposited gold electrodes, we were able to record extracellular signals from the engineered tissue, as well as to control its contraction and release the anti-inflammatory drug dexamethasone. This technology can be built upon to create a variety of degradable devices for tissue engineering of various tissues, as well as pristine cell free devices with electronic components for short-term *in vivo* use.

Supplementary data to this article can be found online at <https://doi.org/10.1016/j.jconrel.2018.05.023>.

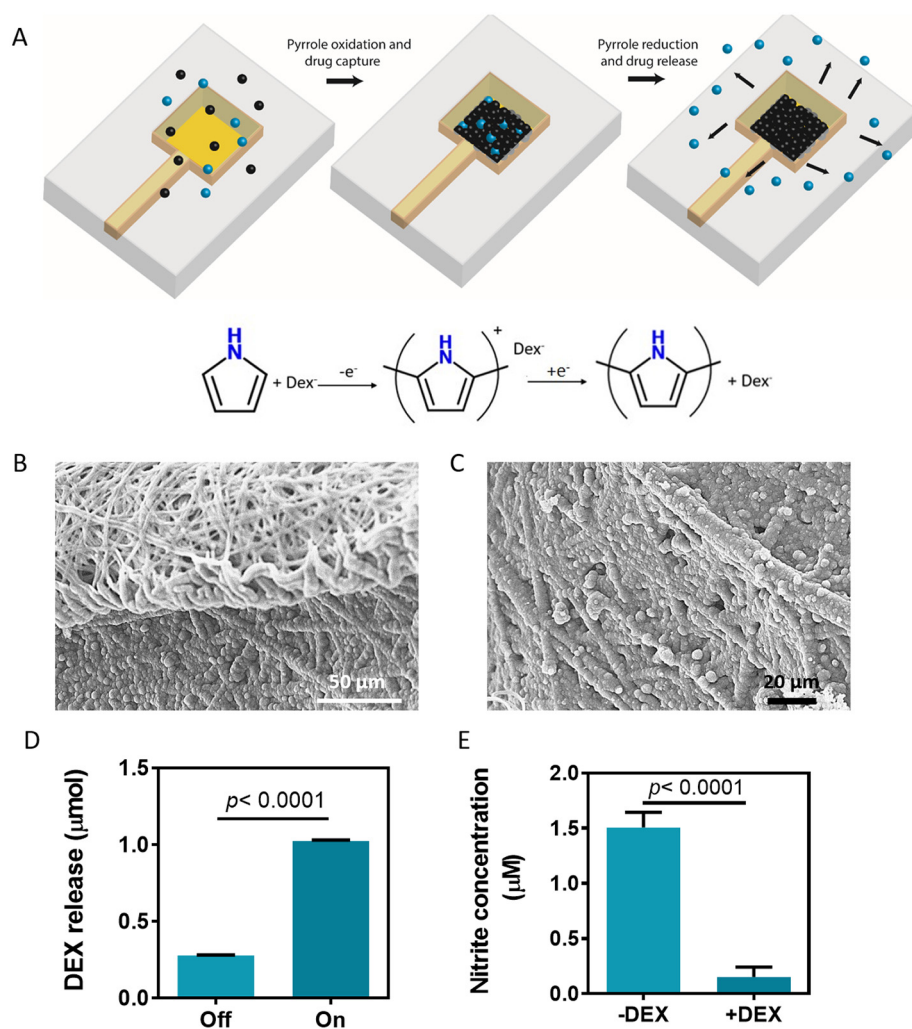


Fig. 5. Controlled drug release. (A) Schematic representation of polypyrrole deposition and dexamethasone release. Pyrrole monomers are oxidized, leading to the deposition of a polypyrrole film with a positive charge, which is balanced by the presence of the negative dexamethasone molecules (top). On the bottom, the chemical process is described. (B) Scanning electron micrograph of the interface between the polypyrrole covered albumin fibers on the bottom and the pristine albumin fibers, serving as a passivation layer. (C) Zoomed-in scanning electron micrograph of the polypyrrole covered albumin fibers. (D) Dexamethasone release from the polypyrrole film with and without an applied voltage. (E) Immune cell function as measured by NO secretion (measured as nitrite, a stable NO metabolite) from activated macrophages.

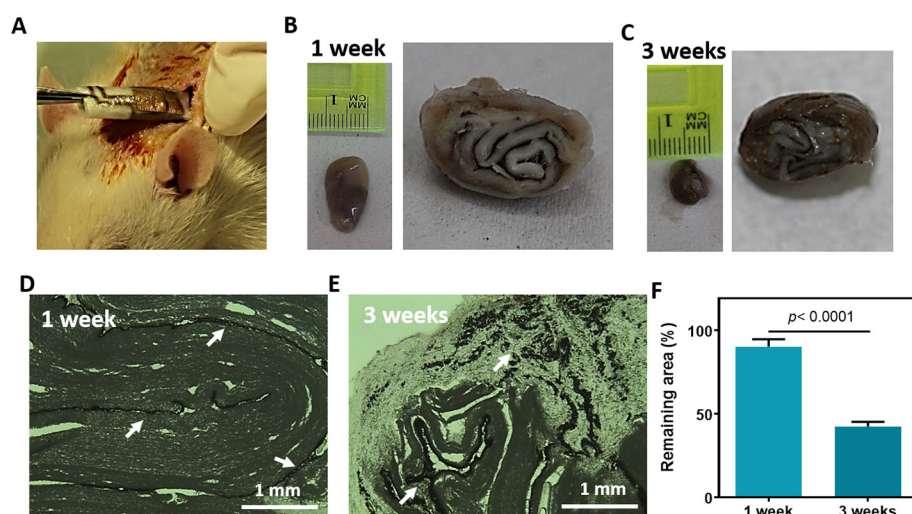


Fig. 6. *In-vivo* degradation. (A) Picture of rolled electronic scaffold implanted subcutaneously into an adult rat. (B and C) Images of the extracted scaffold one week after implantation (B) and 3 weeks post implantation (C). (D and E) Micrograph images of the thin sections of the implants one-week post implantation (D) and 3 weeks post implantation (E). Gold electrodes or their remnants appear in dark brown are indicated by white arrows. (F) Quantification of the remaining scaffold area after extraction. (For interpretation of the references to colour in this figure legend, the reader is referred to the web version of this article.)

Acknowledgment

R.F. and S.F. contributed equally to this work. R.F. was supported by the Clore scholarship program, Marian Gertner Institute for Medical Nanosystems Fellowship and the Argentinian friends of Tel Aviv University. S.F. was supported by the Adams Fellowship Program of the Israel Academy of Sciences and Humanities. T.D. acknowledges support

from European Research Council (ERC) Starting Grant 637943, the Slezak Foundation, and the Israeli Science Foundation (700/13). The work is part of the doctoral thesis of R.F. at Tel Aviv University.

References

[1] R. Feiner, L. Engel, S. Fleischer, M. Malki, I. Gal, A. Shapira, Y. Shacham-Diamond,

- T. Dvir, Engineered hybrid cardiac patches with multifunctional electronics for online monitoring and regulation of tissue function, *Nat. Mater.* 15 (2016) 679.
- [2] B. Tian, J. Liu, T. Dvir, L. Jin, J.H. Tsui, Q. Qing, Z. Suo, R. Langer, D.S. Kohane, C.M. Lieber, Macroporous nanowire nanoelectronic scaffolds for synthetic tissues, *Nat. Mater.* 11 (2012) 986.
- [3] R. Feiner, T. Dvir, Tissue–electronics interfaces: from implantable devices to engineered tissues, *Nat. Rev. Mater.* 3 (2017) 17076.
- [4] A.N. Lukyanov, W.C. Hartner, V.P. Torchilin, Increased accumulation of PEG–PE micelles in the area of experimental myocardial infarction in rabbits, *J. Control. Release* 94 (2004) 187–193.
- [5] Z. Fan, M. Fu, Z. Xu, B. Zhang, Z. Li, H. Li, X. Zhou, X. Liu, Y. Duan, P.-H. Lin, Sustained release of a peptide-based matrix Metalloproteinase-2 inhibitor to attenuate adverse cardiac remodeling and improve cardiac function following myocardial infarction, *Biomacromolecules* 18 (2017) 2820–2829.
- [6] Z. Fan, Z. Xu, H. Niu, N. Gao, Y. Guan, C. Li, Y. Dang, X. Cui, X.L. Liu, Y. Duan, An injectable oxygen release system to augment cell survival and promote cardiac repair following myocardial infarction, *Sci. Rep.* 8 (2018) 1371.
- [7] D.-H. Kim, Y.-S. Kim, J. Amsden, B. Panilaitis, D.L. Kaplan, F.G. Omenetto, M.R. Zakin, J.A. Rogers, Silicon electronics on silk as a path to bioresorbable, implantable devices, *Appl. Phys. Lett.* 95 (2009) 133701.
- [8] D.-H. Kim, J. Viventi, J.J. Amsden, J. Xiao, L. Vigeland, Y.-S. Kim, J.A. Blanco, B. Panilaitis, E.S. Frechette, D. Contreras, Dissolvable films of silk fibroin for ultrathin conformal bio-integrated electronics, *Nat. Mater.* 9 (2010) 511.
- [9] S. Moreno, M. Baniasadi, S. Mohammed, I. Mejia, Y. Chen, M.A. Quevedo-Lopez, N. Kumar, S. Dimitrijevič, M. Minary-Jolandan, Biocompatible collagen films as substrates for flexible implantable electronics, *Advanced Electronic Materials*, 1 (2015).
- [10] H. Koga, M. Nogi, Flexible paper electronics, *Organic Electronics Materials and Devices*, Springer, 2015, pp. 101–115.
- [11] S.W. Hwang, J.K. Song, X. Huang, H. Cheng, S.K. Kang, B.H. Kim, J.H. Kim, S. Yu, Y. Huang, J.A. Rogers, High-performance biodegradable/transient electronics on biodegradable polymers, *Adv. Mater.* 26 (2014) 3905–3911.
- [12] A.H. Najafabadi, A. Tamayol, N. Annabi, M. Ochoa, P. Mostafalu, M. Akbari, M. Nikkha, R. Rahimi, M.R. Dokmeci, S. Sonkusale, Biodegradable nanofibrous polymeric substrates for generating elastic and flexible electronics, *Adv. Mater.* 26 (2014) 5823–5830.
- [13] S. Fleischer, A. Shapira, O. Regev, N. Nseir, E. Zussman, T. Dvir, Albumin fiber scaffolds for engineering functional cardiac tissues, *Biotechnol. Bioeng.* 111 (2014) 1246–1257.
- [14] N. Nseir, O. Regev, T. Kaully, J. Blumenthal, S. Levenberg, E. Zussman, Biodegradable scaffold fabricated of electrospun albumin fibers: mechanical and biological characterization, *Tissue Eng. C Methods* 19 (2013) 257–264.
- [15] J.A. Rogers, T. Someya, Y. Huang, Materials and mechanics for stretchable electronics, *Science* 327 (2010) 1603–1607.
- [16] D.-H. Kim, N. Lu, R. Ghaffari, Y.-S. Kim, S.P. Lee, L. Xu, J. Wu, R.-H. Kim, J. Song, Z. Liu, Materials for multifunctional balloon catheters with capabilities in cardiac electrophysiological mapping and ablation therapy, *Nat. Mater.* 10 (2011) 316.
- [17] D.-H. Kim, N. Lu, R. Ma, Y.-S. Kim, R.-H. Kim, S. Wang, J. Wu, S.M. Won, H. Tao, A. Islam, Epidermal electronics, *Science* 333 (2011) 838–843.
- [18] M. Shevach, B.M. Maoz, R. Feiner, A. Shapira, T. Dvir, Nanoengineering gold particle composite fibers for cardiac tissue engineering, *J. Mater. Chem. B* 1 (2013) 5210–5217.
- [19] M. Shevach, S. Fleischer, A. Shapira, T. Dvir, Gold nanoparticle-decellularized matrix hybrids for cardiac tissue engineering, *Nano Lett.* 14 (2014) 5792–5796.
- [20] K. Baranes, M. Shevach, O. Shefi, T. Dvir, Gold nanoparticle-decorated scaffolds promote neuronal differentiation and maturation, *Nano Lett.* 16 (2015) 2916–2920.
- [21] S. Fleischer, M. Shevach, R. Feiner, T. Dvir, Coiled fiber scaffolds embedded with gold nanoparticles improve the performance of engineered cardiac tissues, *Nano* 6 (2014) 9410–9414.
- [22] S. Fleischer, A. Shapira, R. Feiner, T. Dvir, Modular assembly of thick multifunctional cardiac patches, *Proc. Natl. Acad. Sci.* (2017) 201615728.
- [23] M. Shevach, R. Zax, A. Abrahamov, S. Fleischer, A. Shapira, T. Dvir, Omentum ECM-based hydrogel as a platform for cardiac cell delivery, *Biomed. Mater.* 10 (2015) 034106.
- [24] D. Allen, S. Kurihara, The effects of muscle length on intracellular calcium transients in mammalian cardiac muscle, *J. Physiol.* 327 (1982) 79–94.
- [25] M. Carlsson, P. Cain, C. Holmqvist, F. Stahlberg, S. Lundback, H. Arheden, Total heart volume variation throughout the cardiac cycle in humans, *Am. J. Phys. Heart Circ. Phys.* 287 (2004) H243–H250.
- [26] R. Close, Dynamic properties of mammalian skeletal muscles, *Physiol. Rev.* 52 (1972) 129–197.
- [27] S. Tsurufuji, K. Sugio, F. Takemasa, The role of glucocorticoid receptor and gene expression in the anti-inflammatory action of dexamethasone, *Nature* 280 (1979) 408.